Engineering Geology 304 (2022) 106681

Contents lists available at ScienceDirect

Engineering Geology

journal homepage: www.elsevier.com/locate/enggeo

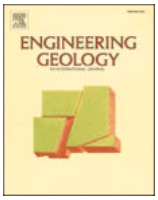

The design of infrastructures in stiff jointed clay formations: A step towards a geological-geotechnical integrated approach

Giuseppe Scarpelli, Viviene M.E. Fruzzetti, Paolo Ruggeri *

Department of Materials, Environmental Sciences and Urban Planning (SIMAU), Università Politecnica delle Marche, Ancona, Italy, Via Brecce Bianche, Ancona, Italy

ARTICLE INFO

Keywords:
Complex formations
Stiff jointed clays
Landslides hazard
Eurocode 7
Geological model
Geotechnical design model
Embedded retaining walls

ABSTRACT

Due to its geological evolution the Mediterranean area is largely characterized by complex and weak formations. These formations make vulnerable and landslide prone many regions of the Mediterranean countries, with the consequence to expose vital infrastructures, as transportation system and lifelines, to unavoidable hazards. Recent developments in the geological field have given a comprehensive description of the processes that have originated these formations as well as the main features of this wide class of materials such as mélanges, hard soils and structurally complex formations. Differently, the translation into engineering terms of many geological aspects is still very limited and the designer is often left alone when he has to conceive a geotechnical design model (GDM) capable of capturing the design situation and the geotechnical properties of complex formations as relevant for design. Considering the operative framework outlined by the draft version of the new European code for geotechnical design (EC7), this paper presents a conceptual approach that can be followed when designing an embedded retaining structures in Stiff Jointed Clay (SJC), a specific sub-group of the complex formations, frequently affected by landslides, where, likewise in rocks, the scale effect strongly influences the selection of the representative ground properties. In particular, based on a prototype numerical model of a SJC formation implemented for one system of discontinuities, the paper will show the close relationship between the geometrical arrangement of the discontinuities, the geometry of the potential collapse mechanisms and the operational strengths to be used in the calculation models. The data from monitoring of a real case study are promising in the appropriateness of the proposed approach, despite the simplicity of the conceptual and calculation models adopted.

1. Introduction

The design of a geotechnical structure or infrastructure is strongly influenced by the geology of the environment in which it is to be built. This is particularly true when the geological setting is characterized by complex and weak formations, a wide class of materials whose behaviour, according to Crosta et al. (2021), cannot be easily interpreted or predicted using only the basic laws of either Soil or Rock Mechanics. Such definition agrees very well with the "geotechnical oriented" definition of Croce (1977) that introduced the "structurally complex formations", as geological formations that cannot be simply modelled as a continuum due to their complicated lithological and structural features. These formations are frequently encountered in the Mediterranean area because of the tectonic processes that have contributed to determining the current conformation of the territories (Carminati et al., 2021) and have a relevant impact for the safety and development of geotechnical works and infrastructures because of their landslide prone nature.

The definition of complex formations is not straightforward and in the past decades many authors proposed different classifications and terminologies (Ogniben, 1953; Selli, 1962; Abbate and Sagri, 1970; Raymond, 1984). Recent developments in the geological field have tried to re-organize the entire matter by means of an accurate description of the processes that have originated these formations as well as the main features of many complex formations (especially melanges, see the comprehensive review of Ogata et al., 2021) that could be linked to geotechnical properties. However, the translation into engineering terms of many geological aspects is still very limited and the designer is often left alone when he has to conceive a geotechnical design model able to capture the design situation and the geotechnical properties of complex formations as relevant for design.

Under a geotechnical perspective, the complexity can derive from the inherent heterogeneity of the ground and/or the presence of

* Corresponding author.
E-mail address: p.ruggeri@staff.univpm.it (P. Ruggeri).

https://doi.org/10.1016/j.enggeo.2022.106681
Received 22 February 2021; Received in revised form 11 March 2022; Accepted 24 April 2022
Available online 27 April 2022

discontinuities and the work of Esu (1977) with his comprehensive classification of structurally complex formations, still represent a reference on the subject. D'Elia et al. (1998) added to the classification by Esu the aspect of the scale of the problem in the evaluation of the geotechnical properties of complex formation, by distinguish the laboratory sample scale (mesostructure) from the scale of engineering problems (macro and/or megastructure). Also, from an engineering perspective, the distinction between a complexity related to the heterogeneity and a complexity related to the structure appears of interest. In the first case the complex formation at the scale of engineering problem appears as a (more or less) chaotic mixture of coarse grains in a finer cohesive matrix. In the second case, it is possible to distinguish a level of organized family of discontinuities that interrupt the mass of the formation. Mélanges is one of the most widespread geologic terms to indicate the first family of complex formations (Ogata et al., 2021) while Stiff Jointed Clay (SJC, D'Elia et al., 1998) represent a relevant subgroup of formations belonging to the second family of complex formations. The two family of complex formations present very different geotechnical properties: in Mélanges, in which organized structures are hard to detect, the response of the geotechnical systems is predominantly dependent on the proportion between the coarse grains and the relatively soft, often clayey, matrix (Wood and Kumar, 2000; Barbero et al., 2012; Kalender et al., 2014; Ruggeri et al., 2016b; Napoli et al., 2018; Napoli et al., 2020; Ruggeri et al., 2021; Shi et al., 2021a; Shi et al., 2021b); differently, in Stiff Jointed Clayey formations, the mechanical behaviour is governed by the "macrostructure" (joints, bedding planes and faults) so that the geotechnical properties of the intact soil are not sufficient to evaluate the behaviour of the geotechnical system (Skempton, 1985; Bromhead, 2013). The relevance of the discontinuities in Stiff Jointed Clays relies on the very low shear strength attained along discontinuities, often close to residual strength value as demonstrated by a number of experimental studies (Marsland and Butler, 1967; Skempton and Petley, 1967; Calabresi and Manfredini, 1973). Having in mind this framework, the investigation in Stiff Jointed Clays should focus on the evaluation of the geotechnical properties of intact soil as well as the shear strength along the discontinuities.

The presence of Stiff Jointed Clay formation makes vulnerable and landslide prone vast regions of the Mediterranean area, so that the design of reliable technical solutions is challenging and requires considerable experience. This is typical with the design and the construction of infrastructural networks that, due to their strict geometrical requirements, imply large earthworks including embankments on natural slopes and underground excavations (Lin et al., 2007; Wang, 2010).

A good example of such issues is represented by the construction of two Italian sections of the European route E90, named as DG21 and DG22, that are parts of the locally called New Ionian National Road (SS106), in the Calabria region (southern Italy).

The European route E90 is part of the network of the corridors identified as relevant by the Europe Union. As represented in Fig. 1, the E90 originates in Lisbon (Portugal), crosses Spain, Italy and Greece and ends in Silopi (Turkey), at the border with Iraq for a total length of about 6442 km. The E90 path of Fig. 1 is superimposed on the map of active faults from Faccenna et al. (2014). By observing the figure, it is evident the frequent crossing of geologically young areas so much affected from active faults. Although complex formations can originate in different geological conditions, Stiff Jointed Clay formations are often encountered in geologically young areas affected by faults, as occurred in the area of the road sections DG21 and DG22.

At the scale of the works, the safety of the infrastructures as well as the prevention of failures in Stiff Jointed Clay largely depends on the correctness of the structural geological model that relies upon the detection of the patterns of discontinuities, requiring a well-suited ground investigation. To this aim, a possible strategy is to adopt the so called "hybrid soil-rock mechanics approach", that is to design a ground investigation that combines the investigation of the intact soil properties by means of laboratory testing (as in classical Soil mechanics) with a careful description of the structural features of the soil mass (as in Rock mechanics, Structural geology and Engineering geology). Even though not expressed in the same terms, some examples of this approach can be found in the works of Burland et al. (1977), Picarelli et al. (2005), Di Maio et al. (2010) and Bromhead (2013).

Based on the data collected during the construction of the two cited road sections DG21 and DG22, the works of Segato et al. (2015) focusing on failure mechanism diagnoses, Ruggeri et al., 2016a focusing on the effectiveness of a deep drainage intervention and Ruggeri et al. (2020) focusing on design strategies to prevent, mitigate and solve instability phenomena have clearly indicated that geometry and kinematics of several instabilities observed during the construction works were governed by the specific geo-structural settings that characterize the slopes involved in the excavations.

In the same framework of the hybrid soil-rock mechanics approach, the present paper promotes a new approach for designing retaining

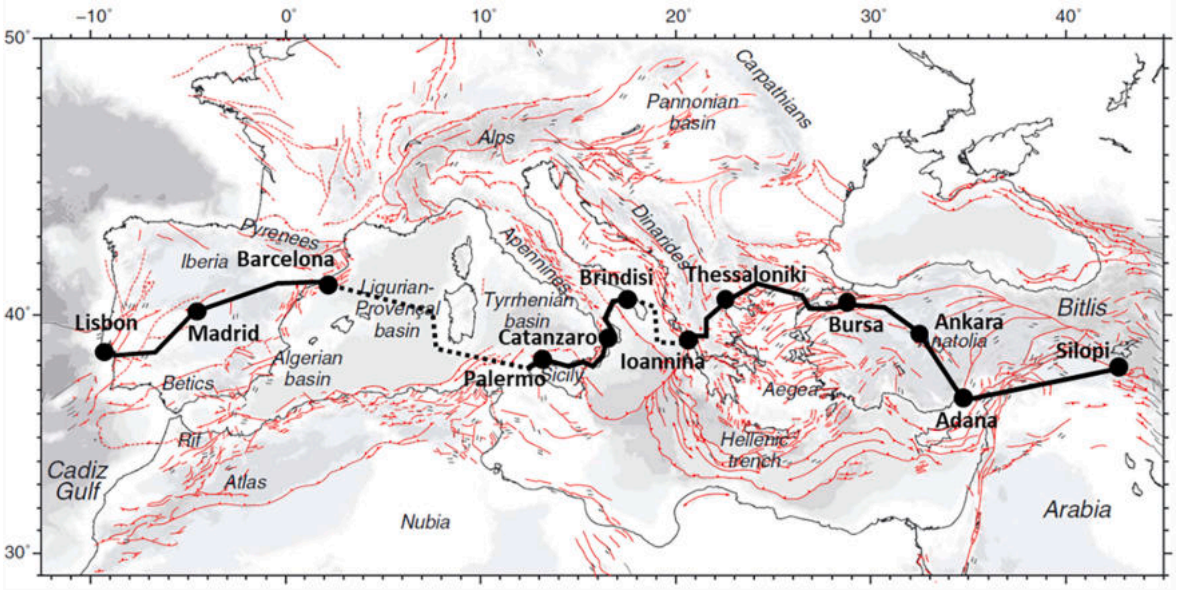

Fig. 1. European route E90 on the map of active faults (modified from Faccenna et al., 2014).

walls in Stiff Jointed Clay suggesting operational estimates of the earth pressures, either active or passive, that account for the influence of the orientation of the discontinuity systems.

This approach was applied to the design of an embedded retaining wall to protect a 6.5 m high excavation located in a slope of Stiff Jointed Clay. The area was not directly affected by landslides, but great caution was imposed considering the proximity to the unstable area that involved the southern portal of a nearby tunnel (Scarpelli et al., 2013). The definition of a simple, but representative, calculation model based on the results of a prototype numerical study was the core of the study to account for the existence of the already well-known pattern of discontinuities.

The paper has also taken into account the provisions of the recent draft of the new Eurocode 7, the most important Code of Design in Europe, that, for the first time, considers the ground complexity as an important ingredient for design. It appears relevant that a new Code, drawn up with the contribution of a large group of technicians and academics representative of European countries, establishes definitions and recommendations for developing a project in the presence of difficult ground conditions, or "ground complexity" as defined in the Code.

Therefore, after a brief presentation of the case study, a suite of bi-dimensional parametric numerical analyses with realistic parameters were developed to investigate the influence of the orientation of one family of discontinuity on the limit values of the soil pressure in a Stiff Jointed Clay. Then, based on the results of the numerical analysis, a geotechnical design model is defined and implemented in a 1D commercial software for design of earth retaining structures. Finally, the comparison between forecasted and monitored displacements of the structure is presented.

Even though the numerical analysis herewith presented is limited to SJC formation affected by only one family of discontinuities, we think that the outlined methodology, based on the identification of the representative geotechnical parameters (for intact soil and discontinuities) and carrying out a parametric numerical analysis to define the operative shear strength of the soil mass, appears to be profitably extended to the study of different design situations in complex formations.

2. The complex formations in the design codes

Design codes are the first reference for engineers dealing with structural and geotechnical design. Therefore, it seems relevant to recognize that even today no guidelines or practical recommendations are given to designers to correctly address problems in complex formations. In this sense it is relevant that the new version of the Eurocodes (also referred as "second generation" of Codes), released in draft form after years of intense work among academics and practitioners all around Europe, includes some recommendations and procedures to address the "ground complexity" in the design of geotechnical work. Note that "ground complexity" is the most general term chosen in the Code to refer to situations in which the geotechnical design should be particularly careful. So, it seems of interest to present the new concepts and procedures outlined in the geotechnical Code when a situation of "ground complexity", as the presence of a complex formation, is encountered.

As pointed out by Estaire et al. (2019), the draft of the new version of Eurocode 7 – Part 1 defines an articulated path for the design of the geotechnical structures that results relevant when a complex formation is encountered. In the Eurocode draft there is a clear distinction between the Ground Model (GM) and the Geotechnical Design Model (GDM). The Ground Model is represented by the "*site specific outline of the disposition and character of the ground and groundwater based on results from ground investigations and other available data*", while the Geotechnical Design Model is defined as the "*physical, mathematical, or numerical representation of the geotechnical system used for the purposes of analysis, design, and verification containing ground information for engineering design purposes developed for a particular design situation and limit state*". It means that a unique Ground Model can generate several Geotechnical Design Models to catch the variety of the ground responses and limit states to consider, as appropriate for any specific geotechnical structure.

Ground complexity enters explicitly in design by classifying possible geotechnical situation into specific "Geotechnical Categories" (GCs). The Geotechnical Category impacts at the level of design (minimum amount of ground investigation, validation of calculation models, designer qualifications and experience, amount of reporting) as well as at the level of activities during construction (minimum supervision, inspection and monitoring).

The Code defines 3 Geotechnical Categories (GC1, GC2 and GC3) as a combination of consequence of failure and geotechnical complexity of the ground and ground-structure interaction. Consequence of failure of a structure is represented by the Consequence Class (CC), classified according to the examples of Table 1.

The geotechnical complexity is defined by classifying the geotechnical structure into one of three Geotechnical Complexity Classes (GCC) – lower, normal or higher – according with the causes of uncertainty described in Table 2. It is relevant to note that "*considerable uncertainty regarding ground conditions*" is indicated as a cause of higher complexity. The combination of the Consequence Class (CC) with the Geotechnical Complexity Class (GCC) gives the Geotechnical Category (GC) according to the Table 3. Among other effects, the Eurocode provides a differentiation of the partial safety factors with the Geotechnical Categories.

Although the Eurocode draft does not account explicitly for complex formations, the introduction of the rock mechanics (totally absent in the previous Code) is probably the most relevant innovation of the new Code because it is now stated the ground properties shall be distinguished when referred to the intact material or to the mass in place. In this sense the clear statement about the influence of the geometry and qualification of the discontinuities on the properties of the rock mass can be easily applied for geotechnical design with Stiff Jointed Clay formations.

3. Infrastructures in a SJC formation: Experiences with DG21 and DG22

The DG21 and DG22 are two new double carriageways road segments, located in the Calabria region (southern Italy), running close to the Ionian coast and interacts mainly with the overconsolidated stiff jointed marine clay sedimentary formation of the Plio-Pleistocene

Table 1
Examples of geotechnical structures with different Consequence Class (CC) from draft of Eurocode 7.

Conseq. Class	Descr. of conseq.	Examples
CC4	Highest	Geotechnical constructions whose integrity is of vital importance for civil protection, earth dams connected to aqueducts and energy plants, levees, tailing dams and earth dams with extreme consequences upon failure (very high risk-exposure), Retaining walls and foundations supporting public buildings, with high exposure.
CC3	Higher	Man-made slopes and cuts, retaining structures with high exposure. Major road/railway embankments, bridge foundations that can cause interruption of service in emergency situations. Underground constructions with large occupancy
CC2	Normal	All geotechnical structures not class. CC1, CC2 or CC4 Retaining walls and foundations supporting buildings with low occupancy.
CC1	Lower	Man-made slopes and cuts, in areas where a failure will have low impact on the society. Minor road embankments not vital for the society. Underground constructions with occasional occupancy.

Table 2
Classification of Geotechnical Complexity Classes (GCC) from draft of Eurocode 7.

Geotech. Compl. Class	Com-plexity	General features causing uncertainty
GCC3	Higher	ANY of the following apply: - considerable uncertainty regarding ground conditions, - highly variable or difficult ground conditions, - significant sensitivity to groundwater conditions - significant complexity of the ground-structure interaction
GCC2	Normal	Covers everything not contained in the features of GCC 1 and 3
GCC1	Lower	ALL the following conditions apply: - negligible uncertainty regarding the ground conditions - uniform ground conditions - standard construction technique - isolated shallow foundations are systematically applied in the zone - well established design methods - low complexity of the ground-structure-interaction.

Table 3
Relationship between Geotechnical Categories (GCs), Consequences Classes (CCs) and Geotechnical Complexity Classes (GCCs) from draft of Eurocode 7.

Consequence Class (CC)	Geotechnical Complexity Class (GCC)		
	Lower (GCC1)	Normal (GCC2)	Higher (GCC3)
Higher (CC3)	GC2	GC3	GC3
Normal (CC2)	GC2	GC2	GC3
Lower (CC1)	GC1	GC2	GC2

epoch.

From a geologic perspective, the area belongs to the Calabrian Arc, a system formed by the superimposition of the Alpine-Betic back-thrust belt remnants over the Apennine Chain during the Tyrrhenian Sea opening. From the late Pliocene to Pleistocene the back-arc zone was affected by extensional tectonics and strike-slip deformation which determined the fragmentation of the Calabrian Arc and the formation of two narrow straits linking the Ionian to the Tyrrhenian sea. The two straits, named Catanzaro and Siderno palaeo-straits, hosted a tidally dominated sedimentation (Longhitano et al., 2012).

The DG21 is a road segment of about 17 km, part of E90 highway, was built between 2007 and 2012, located close to the Catanzaro city. The area falls in the Catanzaro Basin where a 100 m Plio-Pleistocene marly clay unit is encountered, generally under Quaternary deposits that thicken at the foot of the slopes and in the valleys.

The DG22 is a road segment of about 11 km, still part of E90 highway, that lies in the Siderno Palaeo-Straits area. Here the Plio-Pleistocene sedimentary sequence filling the zone, known as Trubi formation, consists of an overconsolidated marly clay and silty clay with sand. Over the Trubi formation it is present a Pleistocene deposit, called "Monte Narbone" formation, mainly formed by slightly cemented sand and gravel. In the valleys, Quaternary deposits of alluvial origin, mainly coarse grained, are encountered.

Due to the hilly morphology of the area, a number of bridges, tunnels, embankments and excavations are required to fulfil the geometric prescriptions of high-speed roads. Such extensive works caused the activation of several soil movements that sometimes progressed up to true instabilities and the dislocation of soil volumes ranging from tens to thousands cubic meters as well as triggering or re-activation of landslides. The back analysis of the events allowed to identify two main groups: shallow instabilities, involving the colluvial-eluvial covers and deep mass movements, in which the surface of rupture take place inside the formation. According to the classification proposed by Hungr et al. (2014) the shallow instabilities belong to the clay/silt planar slide with the sliding surface corresponds to the passage from the eluvial-colluvial cover to the intact formation.

Differently, the deep mass-movements involved the jointed stiff clay formation and were typically observed where the excavation face and the pattern of discontinuities combined to "unlock" a previously stable soil block of intact material. In other terms, the pattern of discontinuities plays a fundamental role in the failure, as is generally the case in rock mechanics instabilities. However, the strength of intact SJC formation is still in the field of Soil Mechanics so that it is possible to have a compound failure surface mainly governed by the existing discontinuities but locally extending into the intact soil (see also Ruggeri et al., 2020).

4. Geotechnical properties of the stiff jointed clay formation

The Stiff Jointed Clay formation (SJC) has been deeply investigated to understand the causes of the deep mass movements occurred during the construction works of the road. The investigation included boreholes, site testings with piezocone (CPTu) and pressumeter (PMT) and laboratory testings.

To understand the behaviour of SJC formation the evaluation of the geotechnical properties of both intact soil and discontinuities resulted essential to apply the presented approach. An overview of the main properties are presented in the following, more details can be found in the work of Vita (2012).

4.1. Geotechnical properties of intact soil

The large number of samples taken to design the different works along the new road allowed to detect that the properties of the SJC formation fall in a narrow range irrespectively of the location of the boreholes.

Typically, values of the unit weight (γ) are between 19 and 21 kN/m^3 and OCR >10.

As shown in Fig. 2a the soil grading curves indicate 40–60% of clay, 40–50% of silt and 0–10% of sand; the liquid limit ranges between 40 and 75 and the Plasticity Index assumes values between 20 and 40, so that the soil can be mainly classified as clay of high plasticity (CH), according to the USCS classification chart of Fig. 2b.

The natural water content (W) is practically constant with the depth and assumes values between 20 and 25%. This corresponds to a void index between 0.6 and 0.7.

The effective strength of the intact soil was evaluated by two different apparatuses: direct shear and triaxial compression tests. The results of direct shear tests on Mohr-Coulomb plane (Fig. 2c) indicate that a linear effective strength envelope can be adopted with peak friction angle of $\varphi'_p = 27^\circ$ and effective cohesion $c'_p = 30$–60 kPa. Some representative stress-strain curves obtained from the triaxial tests are shown in Fig. 2d in terms of normalized deviatoric stress (q/p') versus axial strain (ε_a). It can be noted the brittle behaviour of the soil, visually confirmed by the appearance of a localized shear band in the pictures of the failed samples.

Some piezocone penetration tests allowed the estimation of the undrained cohesion (cu). As shown in Fig. 2e, the undrained cohesion increases from 200 to 400 kPa in the first 10 m of depth, then it assumes values from 400 to 600 kPa.

Values of elastic modulus can be evaluated from laboratory tests on undisturbed samples or estimated from in-situ testing. In Fig. 2f the results of some pressuremeter tests carried out with Ménard apparatus are presented. Values of pressuremeter modulus (Epm) around 40–60 MPa have been obtained.

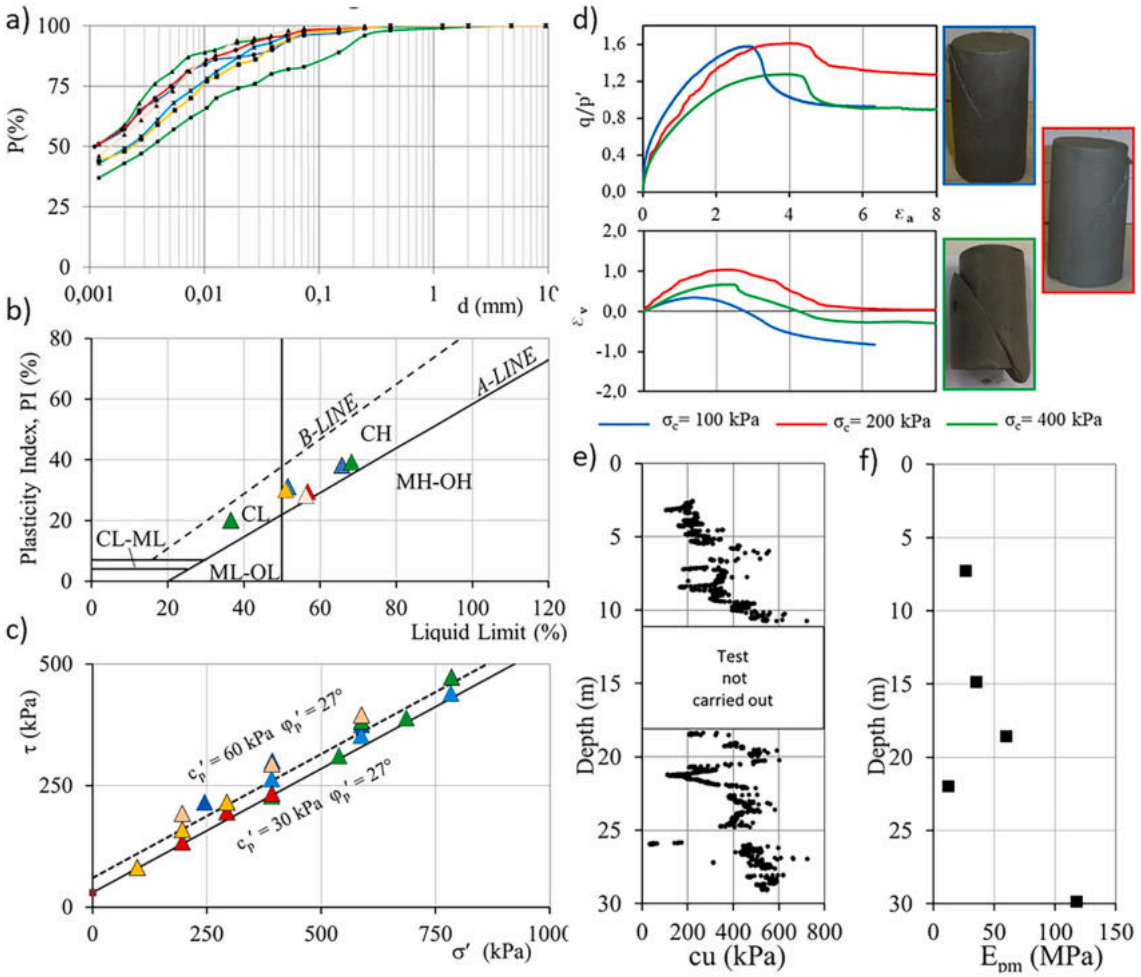

Fig. 2. Typical results from laboratory and in situ testing on intact samples of SJC formation: a) Grain distribution curves; b) Atterberg limits on plasticity chart; c) Results of direct shear tests on Mohr-Coulomb plane; d) Results of triaxial tests; e) Estimation of undrained shear strength from piezocone test; f) Ménard pressuremeter modulus.

4.2. Geotechnical properties along discontinuities

The excavations during the road construction exhumated a number of discontinuities, mainly related to the tectonic setting of SJC formation. The shear strength along such discontinuities was the major issue from an engineering perspective. To investigate such behaviour, a number of direct shear tests on natural samples taken on excavation faces (see Fig. 3a) and containing discontinuities have been carried out. In particular, the tests were carried out by placing, as better as possible, the discontinuity along the sliding plane of the shear test apparatus. For comparison, other direct shear tests at residual, carried out by running several shearing cycles, were carried out starting from undisturbed samples and from samples containing artificially smoothed planes. The tests results are summarized in Fig. 3c. Large part of the results agrees with a Mohr-Coulomb failure envelope described by a friction angle of $\varphi'_r = 18–22°$, without significant difference among the three types of samples preparation. In conclusion, a single representative residual friction angle of 20° was considered appropriate for this formation.

5. Lateral earth pressures in a SJC formation with one system of discontinuities: Numerical study

Based on the measured properties of the investigated SJC formation, a prototype numerical model through FEM analysis was set up to investigate the limit pressure distribution, active and passive, under the hypothesis that only one system of discontinuities, with different orientation, affect the formation.

The model considers an infinitely rigid vertical wall, 10 m height (H) in a dry horizontal ground to which a stepwise increasing horizontal displacement is imposed.

Finite element code PLAXIS 2D (Plaxis, 2017) was used to perform the numerical analyses. The retaining wall was modelled by using plate elements and limit states were induced by a rigid horizontal movement of the wall towards its right side.

The dimensions of the model and the distance of the wall from the sides were selected in a way to minimize the effect of the boundaries: 2.0H in y-direction, 5.5H in x-direction, with 2.5H on the left side and 3.0H on the right side of the wall. Left and right boundaries are constrained in the horizontal direction only, whereas displacements are zero at the base of the model.

Some preliminary analyses for a homogeneous soil with a linearly elastic-perfectly plastic constitutive model obeying to the Mohr–Coulomb criterion confirmed the reliability of the adopted model to reproduce the classical solutions for active and passive pressures. Then, several interfaces have been introduced in the soil mass to reproduce the presence of discontinuities.

The imposed displacement steps were chosen in the range of $\delta = 0.2 \div 10\%$ of the wall height H, so that displacements equal to 20–50–100-200-500-750–1000 mm were imposed. As expected, the displacement of the wall needed to reach the passive limit state is largely greater than the one for the active limit state. It resulted that the active and passive earth pressures have been attained at 50 mm (0.5% of H)

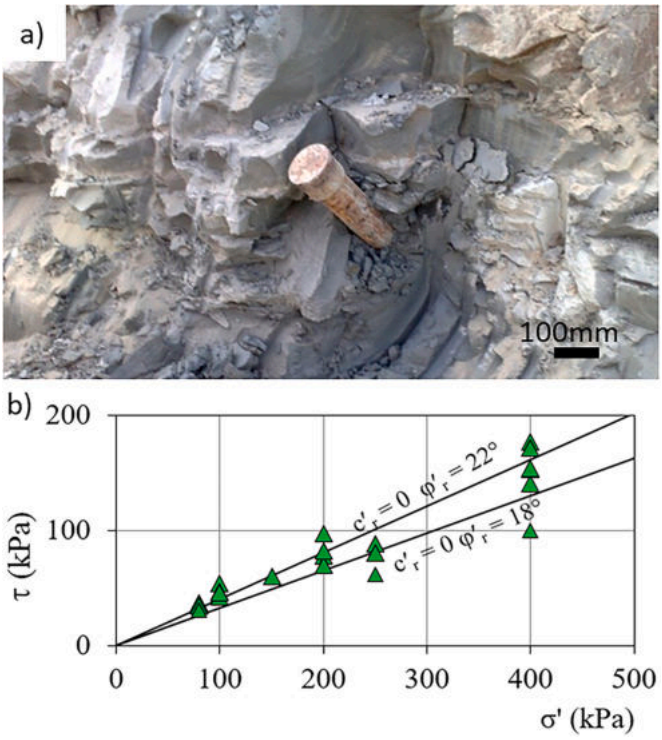

Fig. 3. a) Photo of coring from excavation face through recognized discontinuities; b) Results of direct shear test at residual on Mohr-Coulomb plane.

and 750 mm (7.5% of H) of displacement, respectively.

The soil-wall interface angle (δ) is assumed to be equal to the effective friction angle of the soil (φ'). A specific "interface" element has been introduced to model such interaction. This element allows the detachment of the soil mesh from the wall, improving the quality of the modelling of the soil-structure interaction.

The geotechnical properties assumed for the intact soil are: unit weight 19 kN/m^3, cohesion c' = 30 kPa, friction angle φ' = 27°, elastic modulus E' = 50 MPa, Poisson ratio υ = 0.2. The soil-wall interface is assumed purely frictional, with friction angle φ' = 27°.

The perfectly plastic failure criterion implies the adoption of an associated flow rule as in the classical solutions from limit equilibrium and limit analysis methods. However, the effect of the dilation angle (ψ) should be carefully considered in the numerical modelling, even though the post-peak behaviour of the overconsolidated clay formation has been neglected. This is because a stable unique solution from the numerical model is guaranteed only when an associated flow rule is assumed. For this reason, for the homogenous soil problem, two numerical analyses have been developed considering both a non-associated (ψ = 0) and associated flow rule (ψ = φ). Differently, the analyses on jointed soil mass have been developed assuming the associated flow rule to hold. Note that along the discontinuities a purely frictional behaviour is considered, without any dilation, consistently with the observation of Calabresi and Manfredini (1973) on the mechanical behaviour of stiff clay formation along the joints.

5.1. Classical solutions for lateral pressure for soil formations

Some classical solutions for the earth pressures have been considered as reference to compare the results of the numerical analyses. The at-rest pressure (σ'_{h0}), corresponding to zero wall displacement, is evaluated as:

$$\sigma'_{h0} = K_0\,\sigma'_v \tag{1}$$

where σ'_v is the effective vertical soil pressure at the point of interest and K_0 is the at-rest soil coefficient, as defined below.

The active (σ'_{ha}) and (σ'_{hp}) passive limit values of the soil pressure can be obtained respectively by:

$$\sigma'_{ha} = -2c'\sqrt{K_a} + K_a\,\sigma'_v \tag{2}$$

$$\sigma'_{hp} = +2c'\sqrt{K_p} + K_p\,\sigma'_v \tag{3}$$

in which K_a and K_p represent the active and passive limit coefficients and c' is the cohesion.

Several Authors have proposed different formulations for the at-rest, active and passive limit coefficients. Here, the at-rest soil coefficient has been evaluated according to Jaky (1944) as:

$$K_0 = 1 - sen\varphi' \tag{4}$$

The active limit coefficient has been evaluated according to Coulomb (1776) formulation that, for horizontal ground surface and vertical retaining wall, is expressed as:

$$K_a = \frac{cos^2\varphi'}{cos\delta\left[1+\sqrt{\frac{sin(\varphi'+\delta)sin\,\varphi'}{cos\delta}}\right]^2} \tag{5}$$

in which δ is the friction angle at the soil wall interface. Note that $\delta \neq 0$ implies the inclination of the resultant of the soil pressures against the wall. The horizontal component is then obtained multiplying by the factor cosδ.

The Coulomb solution for the passive limit coefficient becomes unreliable when the interface friction is considered; the analytical solution of Lancellotta (2002) was then adopted. Such solution is relevant because provides a conservative value of passive limit coefficient based on the lower bound theorem of plasticity. The expression of K_p is:

$$K_p = \left[\frac{cos\delta}{1-sin\varphi'}\left(cos\delta + \sqrt{sin^2\varphi' - sin^2\delta}\right)\right]e^{2\theta tan\varphi'} \tag{6}$$

where, beyond the known symbols, there is:

$$2\theta = sin^{-1}(sin\delta/sin\varphi') + \delta \tag{7}$$

Furthermore, considering the relevance of Eurocode 7 for geotechnical design, the K_a and K_p formulas provided by that Code are also considered. Those formulas refer to the work of Kérisel and Absi (1990) on the solutions originally developed by Caquot and Kérisel (1948).

5.2. FEM analysis results on intact soil mass

The results of the numerical analysis for the homogeneous soil example are presented in Fig. 4 in terms of yield points (plastic points status), horizontal displacements and distributions of horizontal pressures against the wall, comparing results for the two cases of non-associated and associated flow-rule. Focusing on the plastic points status, it is possible to distinguish the black points on the left side of the wall, representing Gauss points at failure on the tension cut-off portion of the failure locus, from the red points on the right side of the wall, representing Gauss points where the shear resistance has been fully mobilized (i.e. points where the current stress state falls on the Mohr-Coulomb failure envelope).

The distribution of the plastic points describes very well the failure mechanism activated by the displacement of the wall. Such mechanism is clearly influenced by the soil-wall friction being the deepest sliding curve almost horizontal at the toe of the wall. Moreover, dilatancy considerably influences the extension of the failure mechanism in the passive zone, larger when an associated flow-rule holds, and slightly increases the values of soil pressures.

Focusing on the pressure distributions on the active side of the wall, the numerical analyses well reproduce the expected limit pressures, with values equal to zero to about a depth of 5 m, very close to the critical

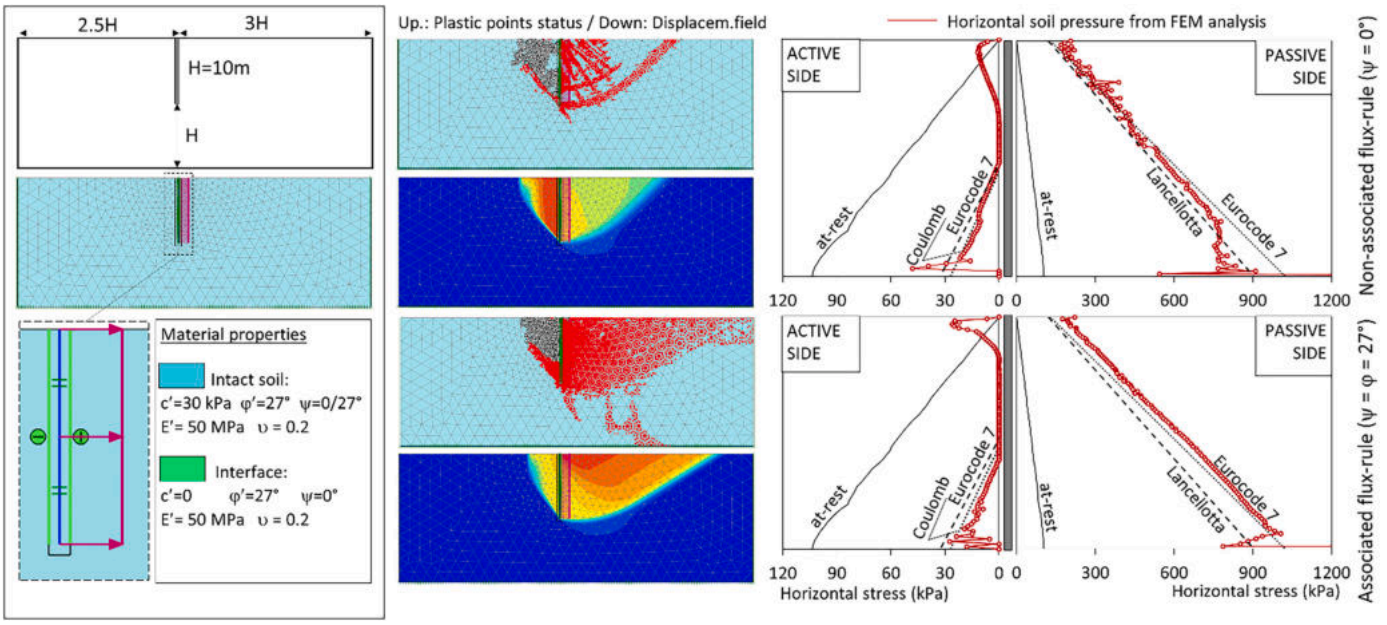

Fig. 4. Numerical analysis of the homogeneous soil model with non-associated (ψ = 0, top half) and associated flow-rule (ψ = φ', bottom half).

height of the unsupported excavation. Beyond this depth, the pressure increases linearly. However, an unexpected increase of the pressures above the critical depth, in the upper part of the wall, was observed. Such trends, probably related to the numerical modelling, are only slightly influenced by the value of the dilatancy assumed in the models and do not affect the general interpretation of the soil pressure on the wall.

On the other hand, the pressures on the passive side are linearly increasing with the depth. Values from the numerical modelling agree very well with the Eurocode 7 solution and are slightly higher than those from the Lancellotta's solution. Moreover, the effect of dilatancy is of a slight increase of the pressures when ψ = φ, when a larger volume of soil is involved in the failure mechanism, although such difference appears irrelevant for engineering purposes. Finally, note that the solution obtained by using an associated flow rule is more stable than when using non-associated one, as it is shown by the fluctuations of the pressure plot in the upper part of the model for ψ = 0.

In conclusion, the good agreement between the soil pressures from the numerical simulations of the homogeneous soil example and classical solutions can be considered as a good reliability test of the considered numerical model.

5.3. FEM analysis results on jointed soil mass

A number of interfaces have been introduced in the soil mass to model the presence of discontinuities. To highlight the effects of the discontinuities on the values of the soil pressures, the presence of a single system of discontinuities, defined by one value of the dip angle (α), was considered in each model. With positive dip direction angle taken clockwise from the horizontal, the following values were assumed: 0°, 30°, 45°, 60°, −30°, −45°, −60°. It is worth to note that positive values of α favour the onset of the active wedge, while negative values of α favour the activation of the passive wedge. To balance the appropriateness of the analysis with time economy, a typical spacing between discontinuities of 2 m has been assumed. A summary of the model schemes and of main results are shown in Fig. 5 in terms of yield points (plastic points status), horizontal displacements and distributions of horizontal pressures against the wall. For each scheme the orientation of the dip angle is shown in the first column of the figure. As reference, the limit earth pressures, from classical solutions of literature for the homogenous soil case, are also plotted.

First, it is evident the great influence of discontinuities and of their respective orientation on the distribution of plastic points and on the geometry of the failure mechanism.

Focusing on active zone, when the discontinuities are horizontal (α = 0) or with negative dip angles (α = −30°, −45°, −60°), the distribution of the plastic points is very similar to that obtained for the homogeneous soil model: the upper part of the model shows a large number of points reaching failure in "tension", essentially mobilising cohesion. On the other hand, when the pattern of discontinuities favours yielding at the active side (α = 30°, 45°, 60°) the failure mechanism becomes a sliding of individual blocks along the discontinuities. This implies that the upward extension of the failure mechanism increases as the dip angle is smaller, but always positive.

The resulting earth pressure distribution on the active side of the wall is again related to the dip angle with pressure values significantly higher than the corresponding values of the homogeneous soil example, whatever is the orientation of the discontinuities (α ≠ 0). This important result was expected for positive dip angles and totally unexpected for the negative ones. The response of the model may be explained with the great influence of the "damage" introduced into the model by the addition of the discontinuities, irrespectively of their orientation. At the scale of engineering works, when evaluating the mechanical response of this specific geotechnical problem, it seems more important to consider the presence of discontinuities rather than the representation of their orientation. This result is probably related to the relatively small shear strength of the intact soil, a situation that differs from that one of rock masses in which the strength of the intact rock is orders of magnitude greater than the strength along the discontinuities.

In Fig. 5, on the active side of the wall, it is also shown the Coulomb earth pressure distribution evaluated for a purely frictional soil with φ' = 27°, that is a soil having the same friction of the intact one and no cohesion. This particular pressure distribution well captures the average trend of the distributions obtained from the numerical analyses with all of the models with discontinuities, especially when their orientations favour collapse against the wall (i.e. α > 0). It is worth noting that the pressure values from the proposed average earth pressure distribution are about 5 times the values obtained adopting the intact soil properties or a soil mass horizontally layered. It means that a retaining wall designed by using the soil properties of the intact soil will be hardly

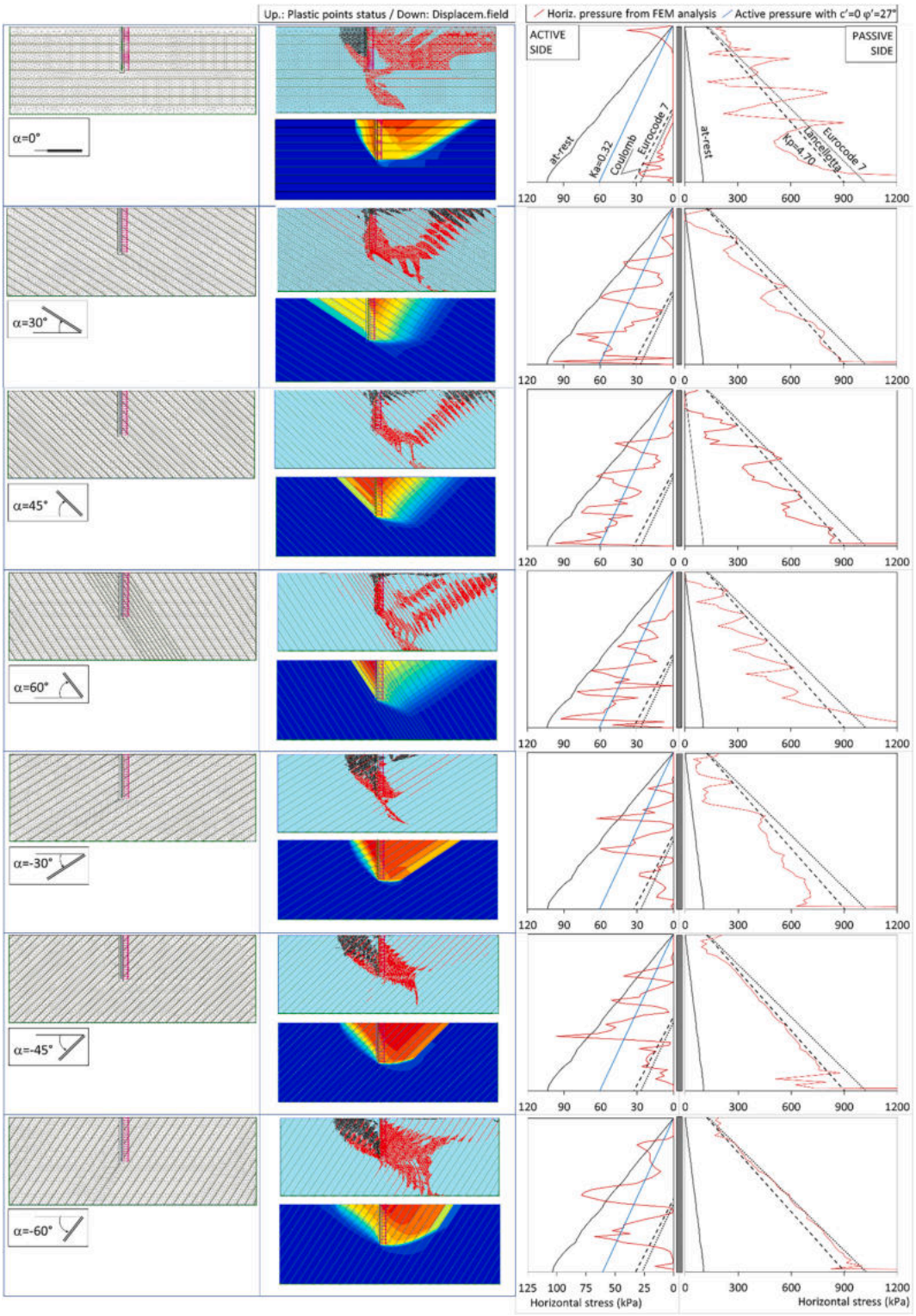

Fig. 5. Results from the calculation models considering joints with variable orientation.

capable at sustaining the earth pressure in the field. Even the adoption of large safety coefficients is ineffective to cover the large gap between expected and real values of the soil pressures.

The severe consequences of the "damage" resulting for the active side of the wall are less evident at the passive side. Of course, the presence of the joints influences shape and extension of the passive resistance mechanism but, in the average, soil pressure distributions does not seem to differ strongly from the theoretical solutions for the homogeneous soil. At first glance, it can be assumed that a 20% reduction of the ground pressures available at the passive side covers the strength reduction even in the worst-case scenario being modelled.

In conclusion, results from the numerical modelling of an ideal rigid wall immersed in a single-system discontinuous ground have shown that the existence of joints in a cohesive-frictional soil mass determines a severe increase of active earth pressures and a minor reduction of the passive resistances. In the specific ideal scenario being analysed, it

seems that an active earth pressure estimated neglecting the contribution of the cohesion may lead to a safe design of the retaining wall.

6. The case study

To protect the uphill side of the excavation needed to connect a tunnel entrance to a bridge along the DG21 road segment, the construction of a retaining wall was planned. The geotechnical design situation had to consider the experience gained for the nearby retaining wall of the tunnel entrance, where large displacements of the top beam were observed (see Fig. 6a) as the consequence of the activation of a mass instability (as clearly demonstrated by the two inclinometer readings shown in Fig. 6b). That experience indicated the need of a more cautious design of the new wall, even if outside of the landslide area, to minimize slope instability risk.

The knowledge acquired to define the remedial measures and complete the construction of the southern portal of the tunnel revealed that the slope was constituted by a SJC formation interested by a pattern of discontinuities not clearly apparent by observing the coring from boreholes. However, by observing the excavation surfaces three main families of discontinuities were distinguished: bedding planes (K1), approximately parallel to the slope surface, and synthetic and antithetic Riedel shear planes (K2s and K2a, respectively). Fig. 7a shows some exemplar pictures of the encountered discontinuities, but details can be found in Scarpelli et al. (2013). The geometrical arrangement of the discontinuities is such that the release of blocks against the wall at the active side becomes kinematically admissible by combining the K1 and K2 systems of discontinuities. Moreover, during the excavation of the tunnel (North-Eastern of the portal), some discontinuities belonging to a minor fault system, not mapped, was clearly encountered. As shown in Fig. 7b and c, it caused the interruption of a yellowish sand layer. This latter system fully justifies the kinematics of the mechanism that caused the activation of the instability at the tunnel portal.

Because of such findings, the design of the new retaining wall, even if moderately high, needed a lot of precautions. The designer proposed to consider the worst possible scenario by adopting the soil strength at residual for the embedded retaining wall. However, the supervisor of the works and the client were not convinced to finance a very expensive solution and required a clear demonstration of the need of a similar scenario.

The plan view of Fig. 8a shows the position of the wall under consideration in relation to the south portal of the tunnel and the activated instability. The height of the excavation ranges from about 6.5 m close to the tunnel entrance to 3.5 m at the end of the wall. The selected structural solution consists of large diameter bored piles (ø1500 mm) spaced 1.80 m with length varying from 18 to 10 m. A robust top beam, with cross section 1.7 × 1.2 m (B × H), completes the wall. In the proximity of the tunnel entrance, where the excavation height is the greatest, few piles have been coupled to increase stiffness and strength of the wall.

A picture of the work taken at the end of construction is shown in Fig. 8b. Note the particular shape of the top beam needed to join the coupled piles and the position of the inclinometer P52, installed in a bored pile to monitor the deformation of the structure. The inclinometer has a length of 18.0 m, so it reaches almost the pile toe. The cross-section n.192 of Fig. 8c shows the pattern of the discontinuities affecting the formation in the volume of influence of the retaining wall.

Previous findings from the prototype numerical modelling guided the definition of the geotechnical design model (GDM) of the embedded retaining wall under consideration. The observed situation resembles

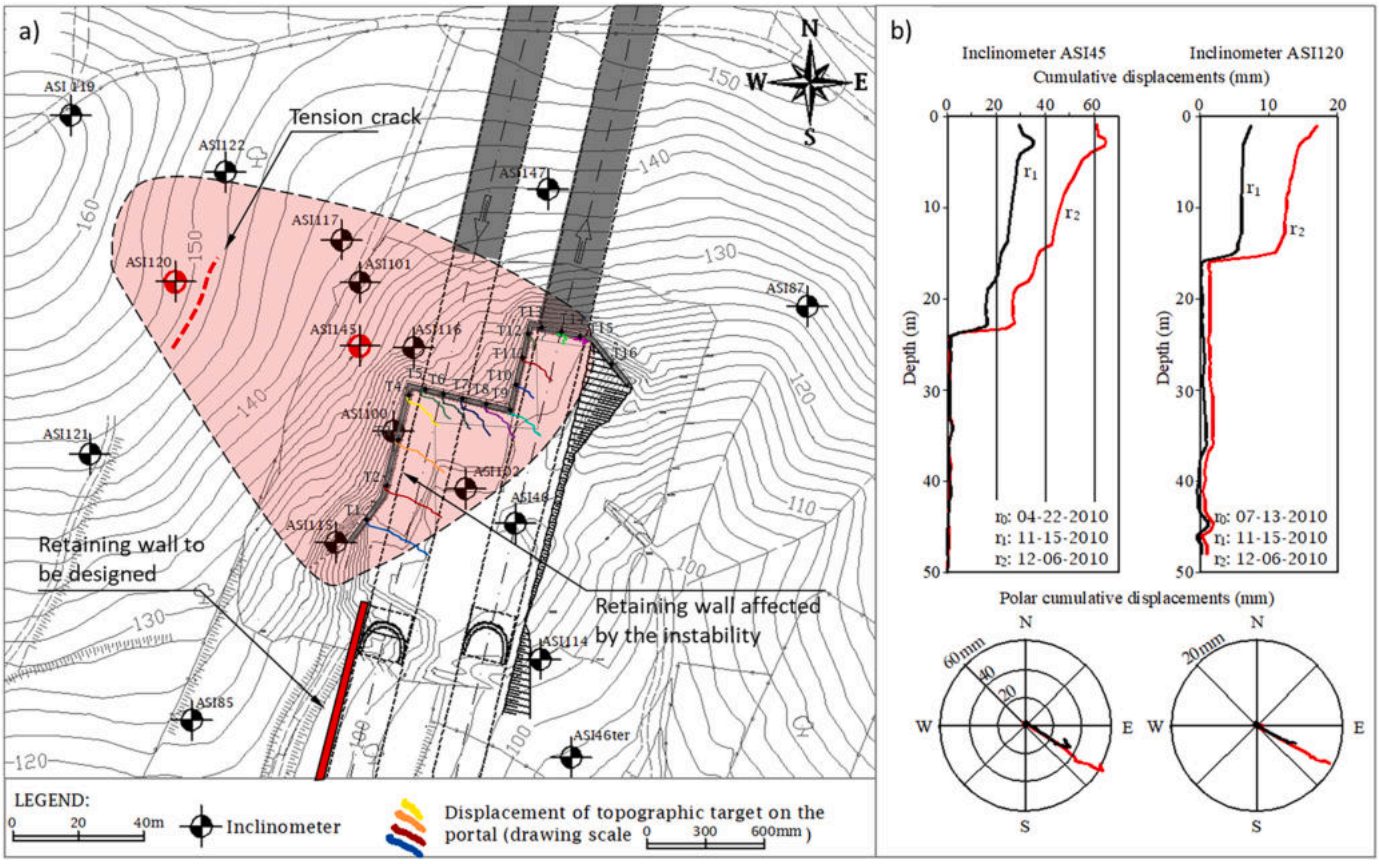

Fig. 6. a) Plan view of the construction site with indication of the activated instability on the tunnel portal, near to the retaining wall to be designed (in red); b) inclinometer readings on the activated landslide. (For interpretation of the references to colour in this figure legend, the reader is referred to the web version of this article.)

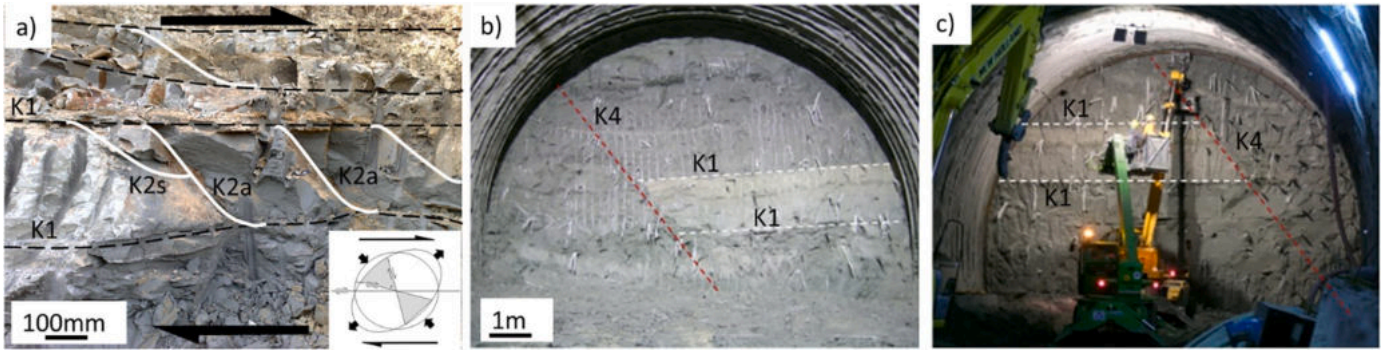

Fig. 7. a) Riedel shear bands detected on an excavation surface; b) Front faces of the twin-tunnel at the same chainage, close to the damaged portal, where the displacement of a yellowish sand layer highlights the presence of a fault zone.

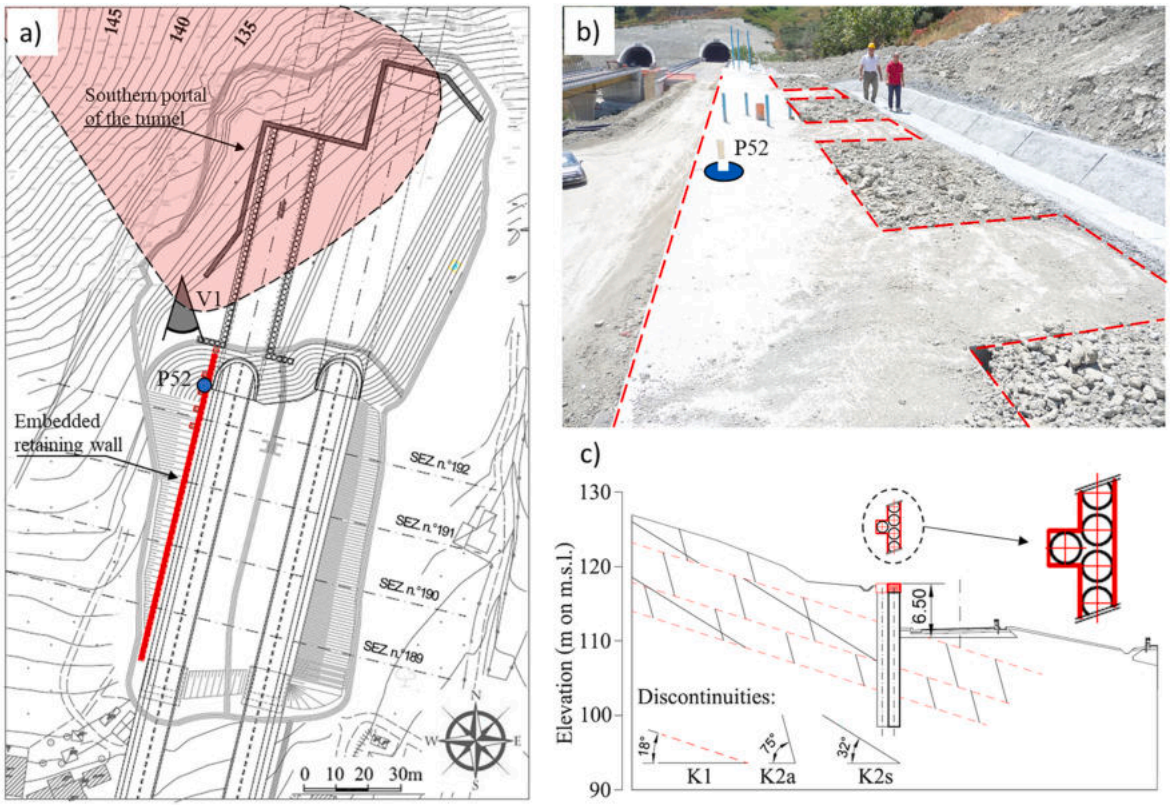

Fig. 8. a) Plan view of the construction site with location of the retaining wall; b) Photo taken soon after construction of the wall, with indication of the inclinometer P52; c) Cross-section n.192 of the wall, with indication of the most relevant discontinuities affecting the slope.

the condition of the prototype model carried out with $\alpha > 0$, that is a condition in which soil pressures at the active side become particularly severe. The situation on the active side of the wall is made even worse by the stress release of the shallow soil layer caused by the inflection of the retaining wall.

In coherence with the findings of the prototype modelling, even though the retaining wall interacts with a single geotechnical unit, the geometrical arrangement of the discontinuities suggests the need of a GDM with geotechnical properties that change from zone to zone around the wall (see also Simpson, 1992). In particular, three different sets of soil strength parameters were used to model the same unit:

- at residual ($c' = 0$ $\varphi' = 20°$) for soil at the active side above the excavation level, where the pattern of discontinuities favour instability and the stress release is more pronounced;
- at critical state ($c' = 0$ $\varphi' = 27°$) for soil at the active side below the excavation level, where the pattern of discontinuities is still unfavourable, but stress release is limited;
- at peak, but considering cautious values, ($c' = 30$ kPa $\varphi' = 27°$) for soil at the passive side of the retaining wall.

As shown in Fig. 9a such GDM has been implemented in a common commercial code, based on the 1D subgrade reaction model (BulkCAD 5.13, 2009), able to carry out an elementary soil structure interaction analysis. The limit values of the coefficient of earth pressures shown in the figure account for the influence of the sloping ground on active earth pressures. At the passive side, considering the results of the numerical prototype model, a slight reduction of the passive limit pressure coefficient has been considered in comparison with the values given by the formulas of Lancellotta or Eurocode 7. The operative Young modulus has been assumed between 50 and 100 MPa.

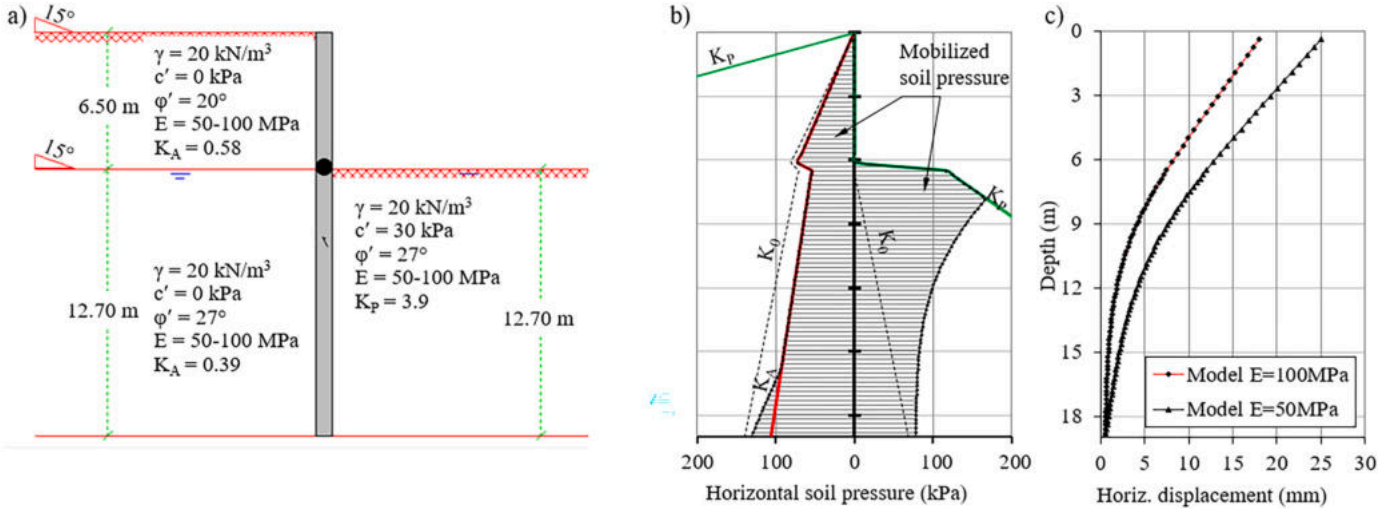

Fig. 9. a) The GDM adopted for designing the embedded retaining wall; results of the numerical analyses: b) mobilized soil pressure on the wall - c) horizontal displacement profiles.

Groundwater table was cautiously assumed at the bottom of the excavation. Such position, more severe than the indication from piezometric monitoring, is an advisable assumption when designing retaining walls in fine grained soils. Moreover, a rack of sub-horizontal drains, located close to the bottom of the excavation, impedes any raise of the groundwater in the whole zone of influence of the geotechnical construction.

6.1. Results of numerical 1D soil-structure interaction analyses

The results of the 1D numerical analysis at the serviceability limit state (SLS) are shown in terms of mobilized soil pressures against the wall (Fig. 9b) and horizontal displacements (Fig. 9c). It can be observed that the active soil pressure is fully mobilized for a large part of the wall except towards its toe where horizontal displacements are not sufficient due to the equilibrium of the wall. On the other hand, the passive soil pressures are entirely mobilized only near to the level of the excavation. The deep soil in the passive zone keeps sufficient resources to equilibrate the wall and ensure the safety margins.

The distributions of the mobilized soil pressures are substantially independent from the value of the Young's modulus adopted for the soil. Instead, the horizontal displacement patterns depend from that value. In Fig. 9c it can be noted the classical deflection of an embedded retaining wall with the maximum value reached at the top. The analysis indicates a maximum displacement between 18 and 25 mm, that is about 0.3% of the excavation hight.

6.2. Monitoring data of the retaining wall

As mentioned before, the embedded retaining wall has been monitored through an inclinometer guide fixed in a bored pile of the segment with maximum height, named P52. The wall has been built between April and May 2012 and the monitoring was carried out from July 2012 to April 2013.

In Fig. 10 the cumulative displacement recorded by the inclinometer is shown. It can be observed that, beyond some experimental errors, the curve matches the typical shape expected for an embedded retaining wall, with the maximum value at the top at the wall. The maximum value of the displacement, equal to 5 mm, is very limited, being lower than 0.1% of H (with H the height of excavation). Such result is in line with the robustness of the retaining wall.

The observed displacement is about 1/3 than that expected from calculation. Such difference is only apparently relevant because of the very limited displacement values we are comparing. Moreover, from an engineering perspective, it is important that the observed displacement is less than the forecast one because it means the modelling assumptions (e.g. real groundwater level probably under the bottom of the excavation) have been cautious without introducing the soil strength at residual everywhere, as considered in the worst case scenario. Moreover, it appears meaningful that this result has been obtained by using a simplified soil structure interaction with a typical commercial code for practitioners.

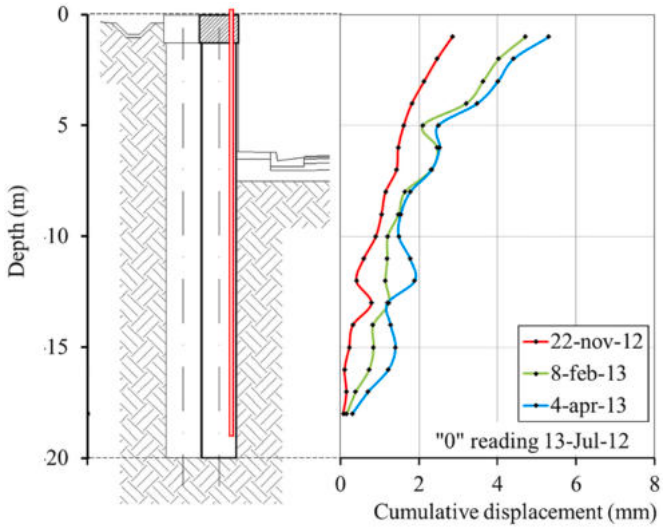

Fig. 10. Inclinometer profiles from the monitoring of P52.

7. Conclusions

For the success of the design the quality of the site investigation is important, with a key role played by geologists and geotechnical engineers, especially when difficult environmental contexts are encountered, as happens with complex and weak formations. In such conditions, the geotechnical engineer has a limited number of tools to rely on and an expert engineering judgement is often not sufficient to build a reliable geotechnical design model capable of preventing the triggering of new instabilities or mitigating the risks associated with existing landslide hazard.

The paper, after a summary of the provisions given by the draft version of the new Eurocode in presence of complex and weak formations, has proposed a methodology that can be applied for design of an embedded retaining wall to protect a road in a landslide prone area in Stiff Jointed Clay formation.

The second generation of the Eurocodes is introducing some new concepts to carry out a geotechnical design in presence of "ground complexity", a general term introduced by the Code able to include complex and weak formations. In particular, the concepts of Consequence Class (CC) and Geotechnical Complexity Class (GCC) contribute to define the Geotechnical Category (GC) that impacts at the level of design as well as at for implementation of design in execution. Among others, a relevant consequence for geotechnical engineers is the differentiation of the partial safety factors with the Geotechnical Categories.

A prototype numerical model, based on realistic properties of a Stiff Jointed Clay formation, has been implemented to evaluate the effect of a single family of discontinuities, with different orientation, on the value of active and passive limit pressure. The results suggest that the existence of joints in a cohesive-frictional ground may produce a severe increase of the active earth pressures and a minor reduction of the passive resistance.

Considering these findings, a retaining wall has been analysed by means of the subgrade reaction model, usually not able to capture the complex behaviour of a stiff jointed ground. For this particular case study, a zoned geotechnical design model is proposed that considers, for the active side, a residual strength zone in the upper ground and a critical friction angle zone in the lower ground, whereas, for the passive resistance only a cautious estimate of the representative values of the geotechnical parameters is suggested.

The comparison between the results of the numerical analysis and the monitoring of the wall proved the safety of the design obtained even if elementary calculation models and design tools for practitioners were used.

In conclusion, to carry out the design of earth retaining structures in Stiff Jointed Clay formations, beyond the groundwater level and the intact soil strength, it is relevant to define the arrangement of discontinuities and the residual strength of soil that resulted to be the key aspects for estimating the limit horizontal stresses of the ground.

Declaration of Competing Interest

The authors declare that they have no known competing financial interests or personal relationships that could have appeared to influence the work reported in this paper.

Acknowledgements

This research was partly funded by Italian Ministry of University and Research, grant number PRIN201572YTLA_005. The authors wish to thank the companies Astaldi S.P.A. and CO.MERI S.P.A. from whose activities originated this research.

References

Abbate, E., Sagri, M., 1970. The eugeosynclinal sequences. In: Sestini, G. (Ed.), Development of the Northern Apennines Geosyncline. Sediment. Geol. 4 (3/4), 251–340.

Barbero, M., Bonini, M., Borri-Brunetto, M., 2012. Numerical simulations of compressive tests on bimrock. Electron. J. Geotech. Eng. 17 (X), 3397–3414.

Bromhead, E.N., 2013. Reflections on the residual strength of clay soils, with special reference to bedding-controlled landslides. Q. J. Eng. Geol. Hydrogeol. 46, 132–156.

BulkCAD 5.13, 2009. User Manual, Concrete S.R.L., Padova, Italy (in Italian).

Burland, J.B., Longworth, T.I., Moore, J.F.A., 1977. 1977 A study of ground movement and progressive failure caused by a deep excavation in Oxford Clay. Geotechnique 27, 557–591.

Calabresi, G., Manfredini, G., 1973. Shear strength characteristics of the jointed clays of *S. Barbara*. Géotechnique 23, 233–244.

Caquot, A., Kérisel, J., 1948. Tables for the Calculation of Passive Pressure, Active Pressure and Bearing Capacity of Foundations. Gauthier-Villars, Paris, p. 1948.

Carminati, E., Petricca, P., Doglioni, C., 2021. Mediterranean tectonics. In: Alderton, David, Elias, Scott A. (Eds.), Encyclopaedia of Geology, Second edition. Academic Press, pp. 408–419. https://doi.org/10.1016/B978-0-08-102908-4.00010-2.

Coulomb, C.A., 1776. Essai sur une Application des Règles des Maximis et Minimis à Quelques Problems de Statique Relatifs à L'architecture, 7. Mém. Math. Phys. Acad. Roy. Sci. par divers Savants, Paris (in French).

Croce, A., 1977. Opening address. In: *Proceedings of the International Symposium: The Geotechnics of Structurally Complex Formations*, Capri, Italy, 19–21 September 1977, II, pp. 148–151.

Crosta, G.B., Picarelli, L., Urciuoli, G., 2021. Slope stability problems in stiff clays and flysch formations, preface to special issue. Ital. Geotech. J. 4 (2021), 5–6.

D'Elia, B., Picarelli, L., Leroueil, S., Vaunat, J., 1998. Geotechnical characterisation of slope movements in structurally complex clay soils and stiff jointed clays. Ital. Geotech. J. 32, 5–47.

Di Maio, C., Vassallo, R., Vallario, M., Pascale, S., Sdao, F., 2010. Structure and kinematics of a landslide in a complex clayey formation of the Italian Southern Apennines. Eng. Geol. 2010 (116), 311–322.

Estaire, J., Arroyo, M., Scarpelli, G., Bond, A.J., 2019. Tomorrow's geotechnical toolbox: Design of geotechnical structures to EN 1997:202x. In: Proceedings of the XVII ECSMGE, Reykjavik, Iceland, 1–6 Sept.

Esu, F., 1977. Behaviour of slopes in structurally complex formations. In: Proceedings of the International Symposium: The Geotechnics of Structurally Complex Formations, Capri, Italy, 19–21 September 1977, II, pp. 292–304.

Faccenna, C., et al., 2014. Mantle dynamics in the Mediterranean. Rev. Geophys. 52, 283–332. https://doi.org/10.1002/2013RG000444.

Hungr, O., Leroueil, S., Picarelli, L., 2014. The Varnes classification of landslide types, an update. Landslides 11 (2), 167–194.

Jaky, J., 1944. The coefficient of earth pressure at rest. J. Soc. Hungarian Archit. Eng. Budapest Hungary 355–358 (in Hungarian).

Kalender, A., Sonmez, H., Medley, E., Tunusluoglu, C., Kasapoglu, K.E., 2014. An approach to predicting the overall strengths of unwelded bimrocks and bimsoils. Eng. Geol. 183, 65–79.

Kérisel, J., Absi, E., 1990. Active and passive earth pressure tables, 1990. Balkema, Rotterdam.

Lancellotta, R., 2002. Analytical solution of passive earth pressure. Géotechnique 52 (8), 617–619.

Lin, M.-L., Chung, C.-F., Jeng, F.-S., Yao, T.-C., 2007. The deformation of overburden soil induced by thrust faulting and its impact on underground tunnels. Eng. Geol. 92 (3–4), 110–132.

Longhitano, S.G., Chiarella, D., Di Stefano, A., Messina, C., Sabato, L., Tropeano, M., 2012. Tidal signatures in Neogene to Quaternary mixed deposits of southern Italy straits and bays. Sediment. Geol. 279, 74–96.

Marsland, A., Butler, M.E., 1967. Strength measurements on stiff fissured Barton Clay from Fawley, Hampshire. In: Proceedings of the Geotechnical Conference, Oslo, Norway, 19–22 September 1967, 1, pp. 139–146.

Napoli, M.L., Barbero, M., Ravera, E., Scavia, C., 2018. A stochastic approach to slope stability analysis in bimrocks. Int. J. Rock Mech. Min. Sci. 101 (November 2017), 41–49. https://doi.org/10.1016/j.ijrmms.2017.11.009.

Napoli, M.L., Milan, L., Barbero, M., Scavia, C., 2020. Identifying uncertainty in estimates of bimrocks volumetric proportions from 2D mesurements. Eng. Geol. 278, 105831 https://doi.org/10.1016/j.enggeo.2020.105831.

Ogata, K., Festa, A., Pini, G.A., Pogacnik, Z., 2021. Mélanges in flysch-type formations: reviewing geological constraints for a better understanding of complex formations with block-in-matrix fabric. Eng. Geol. 293 https://doi.org/10.1016/j.enggeo.2021.106289.

Ogniben, L., 1953. "Argille scagliose" ed "argille brecciate" in Sicilia. Boll. Serv. Geol. Ital. 75, 279–289.

Picarelli, L., Urciuoli, G., Ramondini, M., Comegna, L., 2005. Main features of mudslides in tectonised highly fissured clay shales. Landslides 2005 (2), 15–30.

Plaxis, 2017. Reference Manual for PLAXIS 2D. Plaxis, Delft, Netherlands.

Raymond, L.A., 1984. Classification of melanges. In: Raymond, L.A. (Ed.), Melanges: Their Nature, Origin and Significance, 198. Colorado Geological Society of America Special Papers, Boulder, pp. 7–20.

Ruggeri, P., Fruzzetti, V.M.E., Vita, A., Paternesi, A., Scarpelli, G., 2016a. Deep-seated landslide triggered by tunnel excavation. In: Proceedings of the 12th International Symposium on Landslides, Napoli, Italy, 12–19 June 2016.

Ruggeri, P., Segato, D., Fruzzetti, V.M.E., Scarpelli, G., 2016b. Evaluating the shear strength of a natural heterogeneous soil using reconstituted mixtures. Géotechnique 66 (11), 941–946.

Ruggeri, P., Fruzzetti, V.M.E., Scarpelli, G., 2020. Design strategies to mitigate slope instabilities in structurally complex formations. Geosciences 10, 82.

Ruggeri, P., Fruzzetti, M.E.F., Scarpelli, G., 2021. From ground investigation to the geotechnical model in structurally complex formations. In: Challenges and Innovations in Geomechanics: Proceedings of the 16th International Conference of IACMAG.

Scarpelli, G., Segato, D., Sakellariadi, E., Vita, A., Ruggeri, P., Fruzzetti, V.M.E., 2013. Slope instability problems in Jonica highway construction. In: Landslide Sci. Pract. Risk Assess. Manag. Mitig, 6, pp. 275–282.

Segato, D., Scarpelli, G., Fruzzetti, V.M.E., Ruggeri, P., Vita, A., Paternesi, A., 2015. Excavation works in stiff jointed clay material: examples from the Trubi formation, southern Italy. Landslides 12, 721–730.

Selli, R., 1962. Il Paleogene nel quadro della geologia dell'Italia Centro-meridionale. Mem. Soc. Geol. Ital. 3, 737–789.

Shi, X.S., Liu, K., Yin, J., 2021a. Effect of initial density, particle shape, and confining stress on the critical state behavior of weathered gap-graded granular soils. J. Geotech. Geoenviron. 147 (2) (Article number 04020160).
Shi, X.S., Gao, Y., Ding, J., 2021b. Estimation of the compression behavior of sandy clay considering sand fraction effect based on equivalent void ratio concept. Eng. Geol. 280 (Article number 105930).
Simpson, B., 1992. Retaining structures: Displacement and design. Géotechnique 42, 541–576.
Skempton, A.W., 1985. Residual strength of clays in landslides, folded strata and the laboratory. Géotechnique 35, 3–18.
Skempton, A.W., Petley, D.J., 1967. The strength along structural discontinuities of stiff clays. In: Volume, I.I. (Ed.), Proceedings of the Geotechnical Conference, Oslo, Norway, 19–22 September 1967, pp. 29–46.
Vita, A., 2012. Studio di Una Frana in Terreni Strutturalmente Complessi: Interazione Con Le Opere di Imbocco di una Galleria Stradale. Ph.D. Thesis. Università Politecnica delle Marche (*in Italian*).
Wang, T.-T., 2010. Characterizing crack patterns on tunnel linings associated with shear deformation induced by instability of neighboring slopes. Eng. Geol. 115 (1–2), 80–95.
Wood, D.M., Kumar, G.V., 2000. Experimental observations of behaviour of heterogeneous soils. Mech. Cohesive–Frictional Mater. 5 (5), 373–398.